Generating Synthetic Monthly Net Radiation Data Conditioned On Wind Speed

ABSTRACT

Aims: This study aimed at generating synthetic monthly net radiation data conditioned on wind speed over Port Harcourt, Benue, Kano and Enugu in Nigeria.

Duration of Study: The daily maximum and minimum Relative-Humidity, maximum and minimum air temperature, solar radiation and wind speed data was obtained from the International Institute of Tropical Agriculture (IITA**)** Ibadan, Nigeria for the period of thirty-four (34) years (1977-2010).

Method: The Penman-Monteith (FAO-56) step by step method was used to compute the daily net radiation. The autocorrelation function was used to establish the fact that net radiation and wind speed exhibit the Markov property. Lastly, a two – state Markov Chain model and an indicator function of energy balance and imbalance was developed and used in the course of this work.

Results: The finding reveals that net radiation is surplus over the study areas. The Lag one autocorrelation coefficient confirms the fact that an actual day net radiation and wind speed state depends on the previous day's state. The monthly steady state probabilities of surplus net radiation conditioned on low wind speed is higher compared to monthly steady state probabilities of surplus net radiation conditioned on high wind speed. The indicator function of energy balance or imbalance reveals that there is energy imbalance over study areas.

Conclusion: The generated synthetic net radiation data conditioned on wind speed preserved the characteristics of actual net radiation data when compared as observed in the study. This data is essential in the study of climate change, weather monitoring, agricultural meteorology and estimation of evapotranspiration.

Keywords: Stochastic; Net radiation; Markov Chain; Wind speed.

1. INTRODUCTION

Energy transfer in the atmosphere involves radiation in two different bands of wavelengths: solar radiation emitted by the sun and terrestrial radiation emitted by the earth's surface and atmosphere. The difference between the solar radiation and terrestrial radiation is termed net radiation [1]. This difference creates an adiabatic heat sink over the polar-regions and heat source over the equatorial latitudes. Thus, there is a net transfer of energy from the energy-surplus region of the tropics to the energy-deficit region near the poles in order to maintain steady-state equilibrium within the climate system. Atmospheric wind patterns control how much and where heat energy is released into the atmosphere. This energy is redistributed within the climate system through diverse processes. The climate system tends to remain stable unless the earth experiences a force that shifts the net energy balance. Hence, a shift in the energy balance causes the average earth's surface temperature to become warmer or cooler, resulting in various changes in the atmosphere, on land, and in the oceans [2].

One of the major challenges that researchers in meteorology and climatology are facing all over the world is the development of accurate prediction models. The choice of using a deterministic or a stochastic model depends on the nature of the process to be modeled. Stochastic models take into account the autocorrelation structure of random variables and can also account for the correlation with external variables. The autocorrelation of a random process illustrates the correlation between values of the process at different points in time, as a function of the two times or of the time difference [3]. The nature of the physical processes considered in this research calls for a model with a discrete state in a discrete time stochastic process.

Diverse authors ([4-8]) have estimated net radiation using different methods. [9] and [10] recommended the use of Penman Monteith's (FAO-56) model in computing net radiation given that [11] and [12] encounter difficulties in computing net longwave radiation using the FAO-24 equation. [13] used the First and second order semi-Markov chains for wind speed modeling. [14] predicted the occurrence of surplus and deficit net radiation in Ibadan, Nigeria and [15] investigated the effect of High and Low wind speed on surplus net radiation in Makurdi. Despite the fact that so many researchers model physical processes using the Markov chain model [[16-20]], they did not generate net radiation data conditioned on wind speed over Port Harcourt, Benue, Kano and Enugu, Nigeria. This article proposes the Markov chain model approach to generating synthetic monthly net radiation data conditioned on wind speed over Port Harcourt, Benue, Kano and Enugu, Nigeria. Data generation is very significant in stochastic hydrology and is used by hydrologists for many purposes such as reservoir sizing, water resources, planning, management and climate variability analyses.

1.1 Penman-Monteith's (FAO-56) Model.

The Penman-Monteith's (FAO-56) step by step method was used to compute the daily net radiation and average out monthly. This includes:

The inverse relative distance Earth-Sun (∂r) is given as:

$$\partial r = 1 + 0.033\cos[\frac{2\pi}{365} j] \quad (1)$$

where j is number of the day in the year between 1 (1 January) and 365 or 366 (31 December).

The solar declination (δ) can be found from the approximate equation [1],

$$\delta = 23.45\sin(360\frac{284 + j}{365}) \quad (2)$$

The sun angle (ω_s) is given:

$$\omega_s = \arccos[-\tan(\varphi)\tan(\delta)] \quad (3)$$

where φ is the latitude of a particular location.

The extraterrestrial radiation (R_a), for each day of the year can be estimated using;

$$R_a = \frac{24 \times 3600}{\pi} G_{sc}\partial r(\cos\varphi\cos\delta\sin\omega_s + \frac{\pi\omega_s}{180}\sin\varphi\sin\delta) \quad (4)$$

where G_{sc} is solar constant =1367w/m^2 [1].

The actual vapor pressure (e_a) can be computed [1];

$$e_a = \frac{e_{(T_{\min})}[\frac{RH_{\max}}{100}] + e_{(T_{\max})}[\frac{RH_{\min}}{100}]}{2}.$$

$$e_{(T_{\max})} = 0.6108\exp(\frac{17.27T_{\max}}{T_{\max} + 237.3})$$

$$e_{(T_{\min})} = 0.6108\exp(\frac{17.27T_{\min}}{T_{\min} + 237.3}) \quad (5)$$

where $e_{(T_{\min})}$ and $e_{(T_{\max})}$ are daily saturation vapour pressure at minimum and maximum temperature, and $RH_{\max}$, $RH_{\min}$ are maximum and minimum relative humidity.

The clear-sky radiation R_{so} is given by [1]:

$$R_{so} = (0.75 + 2E10 - 5Z)R_a \quad (6)$$

where *Z* is the elevation above sea level.

The net terrestrial (long wave) radiation (R_T) is proportional to the absolute temperature of the surface raised to the fourth power. This relation is expressed quantitatively by the Stefan-Boltzmann law as given below:

$$R_T = \sigma[\frac{(T_{\max} + 273.16)^4 + (T_{\min} + 273.16)^4}{2}](0.34 - 0.14\sqrt{e_a})[1.35\frac{R_s}{R_{so}} - 0.35] \quad (7)$$

where σ is Stefan-Boltzmann constant [4.903x10^{-9}MJ K^{-4} m^{-2}day^{-1}] and R_s is incoming solar radiation, MJm^{-2} day^{-1}.

Lastly, the net radiation **(** R_n **)** which is the difference between the incoming net shortwave radiation (R_{ns}) and the outgoing net terrestrial radiation (R_T) is given by;

$$R_n = R_{ns} - R_T \quad (8)$$

$$R_{ns} = (1-a)R_s \quad (9)$$

where '*a* 'is albedo = 0.3 [21].

1.2 Autocorrelation

A series of data may have observations that are not independent of one another. Time series are very complex because each observation is dependent upon the previous observation, and is often influenced by more than one previous observation. These influences are called autocorrelations. Autocorrelation coefficients measure correlations between observations at a certain distance apart. An autocorrelation coefficient at lag k can be found by:

$$r_k = \frac{\sum_{i=1}^{N-k}(x_t - \bar{x})(x_{t+k} - \bar{x})}{\sum_{i=1}^{N-1}(x_t - \bar{x})^2} \quad (10)$$

This is the Covariance (x_t, x_{t+k}) divide by the Variance (x_t). A lag is defined as an event occurring at time *'t+k'* (k>0), behind an event occurring at time *'t'* at lag K. The lag one autocorrelation can be specified by matching the conditional probability P (D|D) [22].

1.3 Markov Chain

Markov chain is a stochastic process $\{X_n,\ n = 0,1,2, \ldots \ldots\}$ that takes on a finite or countable number of possible values and if $X_n = i$, then the process is said to be in state i at time n. Supposing that the process is in state i, there is a fixed probability P_{ij} that it will next be in state j. That is;

$$P\{X_{n+1} = j | X_n = i, X_{n-1} = i_{n-1}, \ldots, X_1 = i_1, X_0 = i_0\} = P\{X_{n+1} = j | X_n = i\} = P_{ij} \quad (11)$$

For all states $i_0, i_1, \ldots, i, j$ and $n \geq 0$.

For a first-order Markov chain, the future state X_{n+1} is independent of the previous states $(X_0, X_1, \ldots\ldots, X_{n-1})$, but depends only on the present state X_n [23].

1.4 Transition Probability Matrix

A Markov chain transition matrix is a square array describing the probabilities of the chain transiting from one state to another. This transition probability P_{ij} is given as:

$$P_{ij} = \begin{pmatrix} p_{11} & p_{12} & \cdots & p_{1n} \\ p_{21} & p_{22} & \cdots & p_{2n} \\ \cdots & \cdots & \cdots & \cdots \\ p_{n1} & p_{n2} & \cdots & p_{nn} \end{pmatrix} \quad (12a)$$

The elements P_{ij} are also called stationary probabilities. They are defined by:

$$P(X_n = j / X_{n-1} = i) = p_{ij} \quad (12b)$$

1.5 N-Step Transition Probability Matrix

For any value of n ($n = 2, 3 \ldots$), the n^{th} power of the matrix P specify the probabilities p_{ij}^n that the chain will move from state x_i to x_j is called the n-step probability matrix. This is based on the Chapman Kolmogorov equation, which states as follows;

For any $r \leq n$,

$$P_n = \left(P_{ij}\right)_n = P^{(n)} = \sum_{k=0}^{\infty} P_{ik}^r P_{kj}^{n-r} \quad (13)$$

where P_n denotes the matrix of n-step transition probability [24].

1.6 Steady State Probabilities of a Markov Chain

Consider a Markov chain with Z-states and the row vector

$$\pi = (\pi_1\ \pi_2 \ldots \ldots \ldots \ldots \pi_z) \quad (14)$$

such that

$$\text{(i) } \pi_i \geq 0 \quad \text{(ii) } \sum_{i=1} \pi_i = 1 \quad \text{(iii) } \pi_j = \lim_{n \to \infty} p_{ij}^n \quad (15)$$

where $P\{X_{n+1} = j | X_n = i\} = P_{ij}$,

$(\pi_1\ \pi_2 \ldots \ldots \ldots \ldots \pi_z)$ is called the steady state vector of the Markov Chain. π can be obtained by solving the relation;

$$\pi = \pi P_{ij} \quad (16)$$

where P_{ij} are the stationary probabilities.

2. METHODOLOGY

2.1 Source of Data

The daily maximum and minimum relative humidity, maximum and minimum air temperature, solar radiation and wind speed data was obtained from the International Institute of Tropical Agriculture (IITA**)** Ibadan, Nigeria for the period of thirty-four (34) years (1977-2010).

2.2 Data transformations employed in the modeling process

The daily wind speed and the computed daily net radiation were first transformed into sequence of binary events. The difference between the incoming solar radiation and outgoing terrestrial radiation ought to be zero. When the difference is greater than one or less than one, net radiation is termed surplus or deficit net radiation respectively. For any K^{th} day, a random variable R_{nk} is defined to represent this event, with the realization '0' if the daily net radiation (R_n) is negative (deficit) and '1' if the daily net radiation (R_n) is positive (surplus). A random variable W_k was defined for daily wind speed (W) with realization '0' if 'W' is below average ($\bar{W}$) and '1' if the daily wind speed (W) is above average ($\bar{W}$). This is termed low and high wind speeds respectively. Mathematically we have;

$$R_{nk} = \begin{cases} 0, if\ R_{nk} < 0 \ \text{(deficit net radiation)}. \\ 1, if\ R_{nk} > 0 \ \text{(surplus net radiation)}. \end{cases} \quad (17a)$$

$$W_k = \begin{cases} 0, if\ W_k < \bar{W} \text{(low wind speed)}. \\ 1, if\ W_k \geq \bar{W} \text{(high wind speed)}. \end{cases} \quad (17b)$$

where; $k\ is\ 1, 2, \ldots, n$ (Days), W is daily wind speed and $\bar{W}$ is the average wind speed.

Let $X = \{S/H, S/L, D/H \text{ and } D/L\}$ represent the state space of a four-state (surplus net radiation conditioned by high wind speed, surplus net radiation conditioned by low wind speed, deficit net radiation conditioned by high wind speed and deficit net radiation conditioned by low wind speed) first order Markov Chain. The Markov Chain model for this work is specified as;

$$P(X_{n+1} = j \setminus X_0 = i_0, X_1 = i_1 \ldots, X_n = i_n) = P(X_{n+1} = j \setminus X_n = i_n)$$

for all $(i_0, i_1, \ldots, i_n \in X)$ (18)

where X_{n+1} *is* S/H_{n+1} *or* D/H_{n+1} *or* S/L_{n+1} *or* D/L_{n+1} Conditioned on S/H_n *or* D/H_n *or* S/L_n *or* D/L_n.

The chance of a future state (X_{n+1}) occurring depends only on the immediate past state (X_n). In order to model the relationship between net radiation and wind speed, a new transformation was developed using equations 17*a* and 17*b*. For any K^{th} *day*, a sequence of binary events were captured using a random variable X_k with the realizations '1' if R_{nk} is 1(surplus) and W_k is 1 (high); '2' if R_{nk} is 1 (surplus) and W_k is 0 (low); '3' if R_{nk} is 0 (deficit) and W_k is 1 (high); lastly '4' if R_{nk} is 0 (deficit) and W_k is 0 (low). This process is known as conditioning net radiation on wind speed. This was done daily using the net radiation state (surplus and deficit) and wind speed state (high and low) for each month. Quantitatively, this process is expressed as;

$$X_k = \begin{cases} 1, if\ net\ radiation\ is\ 1\ and\ wind\ speed\ is\ 1\ (S/H)) \\ 2, if\ net\ radiation\ is\ 1\ and\ wind\ speed\ is\ 0\ (S/L)) \\ 3, if\ net\ radiation\ is\ 0\ and\ wind\ speed\ is\ 1\ (D/H)) \\ 4, if\ net\ radiation\ is\ 0\ and\ wind\ speed\ is\ 0\ (D/L)) \end{cases} \quad (19a)$$

It was observed that net radiation is completely surplus over Makurdi, Kano, Port Harcourt and Enugu, Nigeria. Therefore, in order to model the relationship between net radiation and wind speed in these stations, equation (19a) was reduced to:

$$X_k = \begin{cases} 1, if\ net\ radiation\ is\ 1\ and\ wind\ speed\ is\ 1\ (S/H) \\ 2, if\ net\ radiation\ is\ 1\ and\ wind\ speed\ is\ 0\ (S/L)\ . \end{cases} \quad (19b)$$

In this work, the steady-state probabilities for the first order Markov chain model for the four states ($\pi_1,\ \pi_2\ ,\pi_3\ and\ \pi_4$) were determined using the computational formula:

$$\pi_1 = \frac{\pi_2 P_{21} + \pi_3 P_{31} + \pi_4 P_{41}}{1 - P_{11}} \quad ,\pi_2 = \frac{\pi_1 P_{12} + \pi_3 P_{32} + \pi_4 P_{42}}{1 - P_{22}} \quad \pi_3 = \frac{\pi_1 P_{13} + \pi_2 P_{33} + \pi_4 P_{43}}{1 - P_{33}}$$

$$,\pi_4 = \frac{\pi_1 P_{14} + \pi_2 P_{24} + \pi_3 P_{34}}{1 - P_{44}}$$

$$1 = \pi_1 + \pi_2 + \pi_3 + \pi_4 \quad (20a)$$

The steady-state probabilities for the first order Markov chain model for the two states ($\pi_1,\ \pi_2$) were determined using the computational formula:

$$\pi_1 = \frac{p_{01}}{1 + p_{01} - p_{11}}, \quad \pi_2 = 1 - \pi_1\ , \quad \pi_1 + \pi_2 = 1 \quad (20b)$$

where $\pi_1,\ \pi_2\ ,\pi_3\ and\ \pi_4$ are steady-state probabilities of a surplus net radiation conditioned on high wind speed *(S/H),* surplus net radiation conditioned on low wind speed (S/L) , deficit net radiation conditioned on high wind speed (D/H) and deficit net radiation conditioned on low wind speed (D/L) respectively.

The mean recurrence time (in days) for each state is modeled as:

$$1/\pi_1\ ,\ 1/\pi_2\ ,\ 1/\pi_3 \text{ and } 1/\pi_4\ . \quad (21)$$

Due to the huge amount of data involved in this work, a computer program was written in Pascal programming language version 1.5 for obtaining the transition counts, transition probabilities, N-step transition matrix and steady state probabilities.

2.3 Indicator functions of Energy balance.

An indicator function of energy balance and imbalance was developed in this study. Energy balance occurs when the chance of surplus net radiation conditioned on high wind speed equals the chance of surplus net radiation conditioned on low wind speed. Mathematically,

$$I_{Ebc}\ (P) = \begin{cases} Energy\ imbalance\ if \quad (P(S/H) < P(S/L)) \\ \qquad\qquad\qquad\qquad or\ \ (P(S/H) < P(S/L)) \\ \\ Energy\ balance\ if \quad P(S/H) = P(S/L) \end{cases} \quad (22)$$

where $I_{Eb}\ (P)$ is Indicator function of energy balance; $P(S/H)\ and\ P(S/L)$ are probabilities of surplus net radiation conditioned on high and low wind speed.

2.4 Generating net radiation synthetic data conditioned on wind speed.

The monthly retained (not transferred) and transferred net radiation synthetic data was generated using the steady-state probabilities. Mathematically;

$$R_{nr} = P(S/L)x\ R_n$$
$$T_{nr} = P(S/H)x\ R_n \quad (23)$$

where $R_{nr}, T_{nr},\ and\ R_n$ are retained net radiation synthetic data, transferred net radiation synthetic data, and actual value of net radiation.

3.0 RESULTS AND DISCUSSION

Using the Penman-Monteith's (FAO-56) step by step method, average monthly net radiations were computed over Makurdi, Port Harcourt, Enugu and Kano as presented in Table 1. It was observed that monthly net radiation across the study areas were surplus. Surplus net radiation occurs when the amount of solar radiation absorb by the earth surface is greater than the amount of terrestrial radiation emitted. The average monthly wind speed is maximum in June (Makurdi), April (Port Harcourt), March (Enugu and Kano) and minimum in October (Makurdi), December (Port Harcourt), November (Enugu) and December (Kano) as presented in Table 1. However, high wind speeds ought to transfer surplus net radiation from these regions to deficit net radiation regions in order to maintain the climate system in these regions.

Table 1: Average monthly net radiation and wind speed.

	MAKURDI		PORT HARCOURT		ENUGU		KANO	
MONTH	N. R.	W. S.	N. R.	W. S.	N. R.	W. S.	N. R.	W. S.
JAN.	9.61	4.34	9.79	4.21	9.68	4.29	9.68	3.99
FEB.	10.31	4.27	9.98	4.23	10.37	4.56	10.56	4.43
MAR.	9.48	4.26	10.01	4.34	10.44	4.87	11.23	4.92
APR.	10.18	4.25	9.58	4.49	10.21	4.75	11.35	4.84
MAY	10.57	4.28	9.86	4.36	9.95	4.33	11.02	4.45
JUNE	9.94	4.80	10.35	4.40	9.62	4.60	10.33	4.49
JULY	9.82	4.60	10.46	4.47	9.38	4.54	9.92	4.51
AUG.	10.02	4.37	10.52	4.42	9.32	4.42	9.70	4.20
SEPT.	9.70	4.28	10.69	4.44	9.77	4.40	10.17	4.03
OCT.	9.86	4.08	10.32	4.22	9.64	4.55	10.71	3.64
NOV.	10.36	4.41	9.83	4.34	9.61	4.15	10.52	3.60
DEC.	10.16	4.58	9.80	4.07	9.44	4.35	9.40	3.52

N.R.-Net Radiation (MJm^{-2} day^{-1}) W.S. - Wind Speed (m/s)

The Lag one autocorrelation coefficient of net radiation and wind speed across locations confirms the fact that an actual day net radiation or wind speed state depends on the previous day's state. Hence, there is a significant higher autocorrelation between net radiation and wind speed at lag one (p-value < 0.05) than at other lags as presented in Table 2.

Table 2: Lag one autocorrelation coefficient of Net radiation and wind speed.

			BOX-LUNG STATISTIC		
STATION	PARAMETERS	AUTO. COEFF.	VALUE	P-VALUE	REMARK
MAKURDI	Net radiation	0.668	164.377	0.00	Significant
	Wind speed	0.52	99.48	0.00	Significant
PORT HARCOURT	Net radiation	0.635	148.413	0.00	Significant
	Wind speed	0.475	82.036	0.00	Significant
ENUGU	Net radiation	0.799	98.402	0.00	Significant
	Wind speed	0.516	235.75	0.00	Significant
KANO	Net radiation	0.727	194.765	0.00	Significant

Wind speed	0.525	101.788	0.00	Significant

P-Value< 0.05=Significant

The monthly transition probability of net radiation was modeled using the Markov chain approach mentioned in Section 1.4. The monthly first order transition probability matrix is of size 2X2, which is shown in Table 3(a) and 3(b). In Table 3(a) and 3(b), each element shows the probability of the next net radiation conditioned on wind speed state based on the current state. It reveals that the highest probability occurs on the diagonal of the matrix. Consequently, if the current surplus net radiations conditioned on high or low wind speeds state are known, it is most likely that the next state will be in the next category. Surplus net radiation conditioned on low wind speed transiting into the same state has the highest probabilities over Port Harcourt, Makurdi, Enugu and Kano as shown in Table 3(a) and 3(b).

Table 3 (a): Probability Transition Matrix of First Order Markov Chain Model (January to June).

STATIONS	SEQ.	JANUARY		FEBURARY		MARCH		APRIL		MAY		JUNE	
		S/H	*S/L*	*S/H*	*S/L*	*S/H*	*S/L*	*S/H*	*S/L*	*S/H*	*S/L*	*S/H*	*S/L*
MAKURDI	*S/H*	0.60	0.40	0.60	0.40	0.64	0.36	0.61	0.39	0.60	0.40	0.65	0.35
	S/L	0.25	0.75	0.26	0.74	0.28	0.72	0.24	0.76	0.29	0.71	0.24	0.76
ENUGU	*S/H*	0.62	0.38	0.64	0.36	0.67	0.33	0.6	0.4	0.62	0.38	0.59	0.41
	S/L	0.28	0.72	0.27	0.73	0.25	0.75	0.31	0.69	0.31	0.69	0.27	0.73
P/H	*S/H*	0.62	0.38	0.59	0.41	0.64	0.36	0.66	0.34	0.57	0.43	0.65	0.35
	S/L	0.33	0.67	0.27	0.73	0.25	0.75	0.3	0.70	0.29	0.71	0.27	0.73
KANO	*S/H*	0.74	0.26	0.65	0.35	0.68	0.32	0.61	0.39	0.60	0.40	0.56	0.44
	S/L	0.22	0.78	0.29	0.71	0.28	0.72	0.32	0.68	0.32	0.68	0.33	0.67

Table 3 (b): Probability Transition Matrix of First Order Markov Chain Model (July to December).

STATIONS	SEQ.	JULY		AUGUST		SEPTEMBER		OCTOBER		NOVEMBER		DECEMBER	
		S/H	*S/L*	*S/H*	*S/L*	*S/H*	*S/L*	*S/H*	*S/L*	*S/H*	*S/L*	*S/H*	*S/L*
MAKURDI	*S/H*	0.56	0.44	0.61	0.39	0.60	0.40	0.65	0.35	0.62	0.38	0.61	0.39
	S/L	0.29	0.71	0.28	0.72	0.28	0.72	0.28	0.72	0.25	0.75	0.28	0.72
ENUGU	*S/H*	0.66	0.34	0.66	0.34	0.60	0.40	0.67	0.33	0.62	0.38	0.58	0.42
	S/L	0.24	0.76	0.27	0.73	0.26	0.74	0.19	0.81	0.28	0.72	0.27	0.73
P/H	*S/H*	0.66	0.34	0.63	0.37	0.66	0.34	0.57	0.43	0.56	0.44	0.56	0.44
	S/L	0.28	0.72	0.25	0.75	0.22	0.78	0.28	0.72	0.25	0.75	0.34	0.66
KANO	*S/H*	0.59	0.41	0.68	0.32	0.61	0.39	0.61	0.39	0.68	0.32	0.68	0.32
	S/L	0.28	0.72	0.26	0.74	0.28	0.72	0.30	0.70	0.20	0.80	0.22	0.78

S/H – Surplus net radiation conditioned on High wind speed. S/L – Surplus net radiation conditioned on Low wind speed.

Table 4 presents the monthly steady state probabilities of surplus net radiation conditioned on high and low wind speed. Surplus net radiation conditioned on low wind speed has the highest probabilities across study locations. Since the monthly steady state probabilities are not equal, the indicator function of energy balance (section 2.4) reveals that there is energy imbalance in these regions. These imbalances results to complex but organized patterns of energy and water transfer in the atmosphere. It also determines the weather and climate of these regions and greatly moderates the air temperature.

Table 4: Monthly steady state probabilities of surplus net radiation conditioned on high or low wind speed.

	MAKURDI		PORT HARCOURT		ENUGU		KANO	
MONTH	S/H	S/L	S/H	S/L	S/H	S/L	S/H	S/L
JAN.	0.38	0.62	0.47	0.54	0.42	0.58	0.46	0.54
FEB.	0.39	0.61	0.4	0.6	0.43	0.57	0.45	0.55
MAR.	0.44	0.56	0.41	0.59	0.43	0.57	0.47	0.53
APR.	0.38	0.62	0.47	0.53	0.44	0.56	0.45	0.55
MAY	0.42	0.58	0.4	0.6	0.45	0.55	0.44	0.56
JUNE	0.41	0.59	0.44	0.57	0.4	0.6	0.43	0.57
JULY	0.4	0.6	0.45	0.55	0.41	0.59	0.41	0.59
AUG.	0.42	0.58	0.4	0.6	0.44	0.56	0.45	0.55
SEPT.	0.41	0.59	0.39	0.61	0.39	0.61	0.42	0.58
OCT.	0.44	0.56	0.39	0.61	0.37	0.64	0.44	0.57
NOV.	0.4	0.6	0.36	0.64	0.42	0.58	0.39	0.62
DEC.	0.42	0.58	0.44	0.56	0.39	0.61	0.41	0.59

S/H – Surplus net radiation conditioned on High wind speed. S/L – Surplus net radiation conditioned on Low wind speed.

The mean reoccurrence times were evaluated using equation 22, which is the number of days it takes for a given state to reoccur. On the average, it takes 2.44, 2.40, 2.31 and 2.41 days for surplus net radiation conditioned on high wind speed and 1.69, 1.72, 1.77 and 1.72 days for surplus net radiation conditioned on low wind speed to reoccur in Makurdi, Port Harcourt, Kano and Enugu respectively (Table 5). Thus, the weather of Enugu would be hot for 2.41 days and cool for 1.72 days on the average, resulting in harsh and hot weather or climate at the long run. This result further agrees with [25] and possibly explains why Enugu is hot all throughout the year. According to [26], heat waves occur when the maximum temperature of a place is greater than 35^{o}C for 3 days or more consecutively.

Table 5: Monthly mean reoccurrence times (days) across locations.

	MAKURDI		PORT HARCOURT		ENUGU		KANO	
MONTH	S/H	S/L	S/H	S/L	S/H	S/L	S/H	S/L
JAN.	2.63	1.61	2.15	1.87	2.36	1.74	2.18	1.85
FEB.	2.56	1.64	2.52	1.66	2.33	1.75	2.21	1.83
MAR.	2.27	1.79	2.44	1.69	2.32	1.76	2.14	1.88
APR.	2.63	1.61	2.13	1.88	2.29	1.78	2.22	1.82
MAY	2.38	1.72	2.48	1.68	2.23	1.81	2.25	1.8
JUNE	2.44	1.69	2.3	1.77	2.52	1.66	2.33	1.75
JULY	2.5	1.67	2.21	1.82	2.42	1.71	2.46	1.68
AUG.	2.38	1.72	2.48	1.68	2.26	1.8	2.23	1.81
SEPT.	2.44	1.69	2.54	1.65	2.54	1.65	2.39	1.72
OCT.	2.27	1.79	2.54	1.65	2.74	1.57	2.3	1.77
NOV.	2.5	1.67	2.76	1.57	2.36	1.74	2.6	1.63
DEC.	2.38	1.72	2.29	1.77	2.56	1.64	2.46	1.69

S/H – Surplus net radiation conditioned on High wind speed. S/L – Surplus net radiation conditioned on Low wind speed.

The means reoccurrences time reveals that Makurdi, Port Harcourt, Kano and Enugu would be hot for 2.44, 2.40, 2.31 and 2.41 days with an air temperature ranging from 32-37.5°C as presented in Figure 1. Hence, the risk of heat related illness is low for now across these regions because the weather is hot for less than three (3) days and the air temperature varies daily.

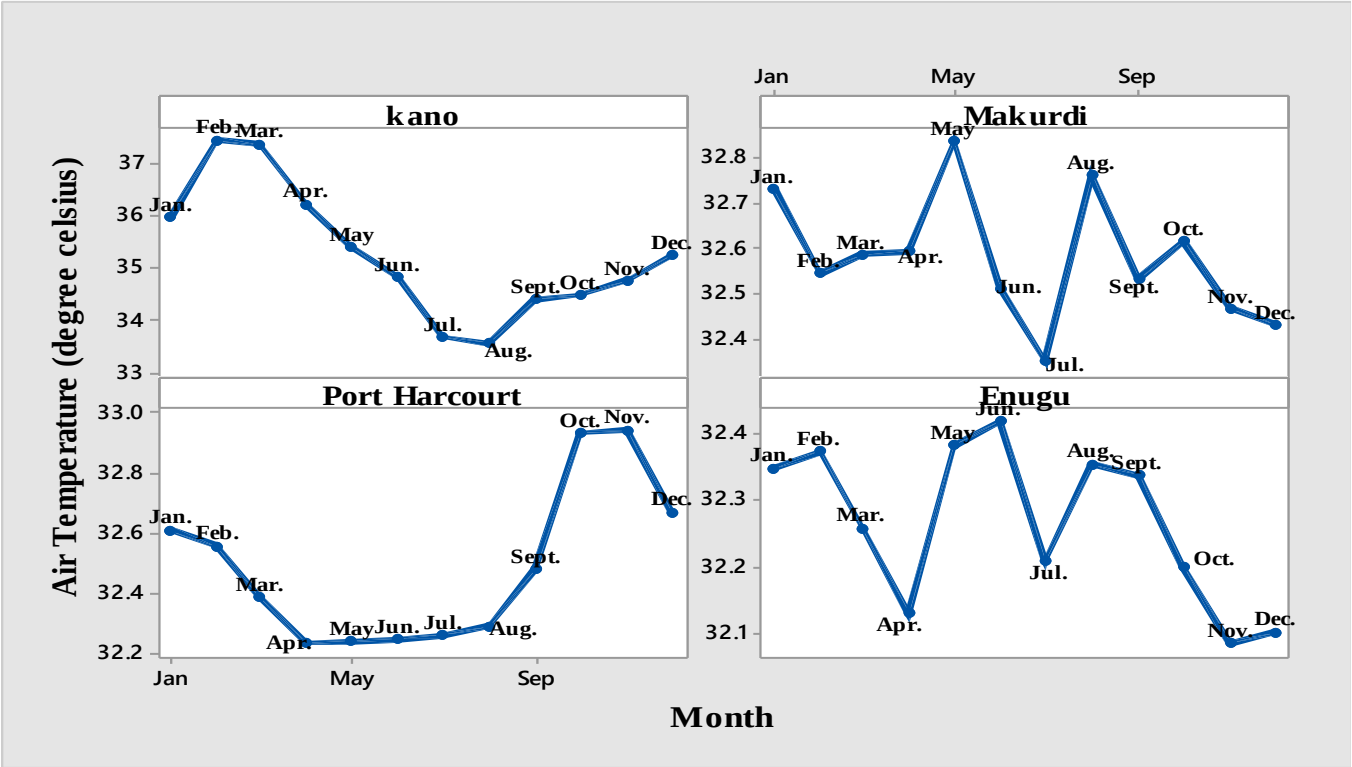

Figure 1: Monthly average air temperature (^{o}C) across locations.

A shift in net radiation can result to a shift in air temperature over Makurdi, Port Harcourt, Kano and Enugu. One of the major indicators of climate change is the increase or decrease of air temperature according to [2]. Warmer temperatures can result to changes in the frequency and size of intense precipitation events, which may in turn affect the frequency and size of river flooding. Makurdi has witnessed the highest frequencies of extreme rainfall events and flood frequencies between the periods of 1996 and 2001 [27]. Bigger or more frequent floods could damage bridges, roads, homes, and other infrastructure; harm or displace people; wipe out farmers' crops; pollute water supplies; and disrupt ecosystems by displacing aquatic life, increasing soil erosion and impairing the quality of water [28]. 40% of the rural inhabitants are committed to agricultural activities in River state. A variety of short season crops including cocoyam, water yam, sweet-potato, groundnut, maize, sugar-cane and assorted vegetables are grown in Port Harcourt [29]. A continuous increase in the air temperature in Port Harcourt can affect all these crops negatively. Warmer air temperatures connected with climate change can increase the mosquito development, incubation of the disease within a mosquito and the biting rates [30] across these study areas. An increase in air temperature can also trigger quite a number of tropical diseases such as célèbre-spinal-meningitis, heat cramps, malaria, heat strokes, and so on [31].

Table 6: Synthetically generated monthly net radiation data conditioned on high and low wind speed

Months	Makurdi		Kano		Port Harcourt		Enugu	
	T_{nr}	R_{nr}	T_{nr}	R_{nr}	T_{nr}	R_{nr}	T_{nr}	R_{nr}
January	3.652	5.958	4.435	5.249	4.555	5.240	4.102	5.573
February	4.021	6.289	4.784	5.777	3.964	6.020	4.451	5.924
March	4.171	5.309	5.242	5.983	4.106	5.908	4.501	5.943
April	3.865	6.305	5.120	6.232	4.495	5.089	4.463	5.750
May	4.435	6.125	4.891	6.125	3.972	5.884	4.469	5.484
June	4.075	5.865	4.433	5.901	4.501	5.846	3.821	5.803
July	3.928	5.892	4.027	5.892	4.726	5.730	3.883	5.497
August	4.208	5.812	4.344	5.353	4.241	6.283	4.127	5.190
September	3.977	5.723	4.250	5.917	4.200	6.487	3.850	5.922
October	4.334	5.516	4.657	6.049	4.066	6.254	3.517	6.119
November	4.144	6.216	4.048	6.467	3.558	6.272	4.076	5.538
December	4.267	5.893	3.826	5.574	4.271	5.525	3.690	5.748

Table 6 shows the synthetically generated monthly net radiation data conditioned on high or low wind speed across locations. This was achieved using equation 23 under section 2.4. The amount of surplus net radiation ($MJm^{-2}day^{-1}$) retained (R_{nr}) over Makurdi, Port Harcourt, Kano and Enugu is higher compared to the amount of surplus net radiation transferred (T_{nr}). The wind speed is so low (Table 1) to transfer all the surplus net radiation from these locations, thereby resulting in an increase in the air temperature in these locations.

5.0 Conclusion

This paper presents a first order Markov chains model to syntactical generate monthly net radiation data conditioned on high or low wind speed over Makurdi, Port Harcourt, Kano and Enugu, Nigeria using a 34-years (1977-2010) real time weather data. The results show that the synthetic net radiation data conditioned on high or low wind speed (Table 6) preserved the characteristics of actual net radiation data (Table 1). The most important benefit of this method is that the synthetic generated data can be helpful in the study of weather monitoring, agricultural meteorology, climate change, energy transfer between two regions and evapotranspiration. One of the greatest ambiguities in modeling climate data under climate change state is the uncertainty in future climate predictions. Thus, if future climate state is known with adequate accuracy, the Markov Chain model available now can be adapted to generate climate data for the new state.

References

[1] Lincoln Z, Michael DD, Consuelo CR, Kati WM, Kelly TM. Step by Step Calculation of the Penman-Monteith Evapotranspiration (FAO-56 Method). *Journal of Agricultural and Biological Engineering.* 2015;1-10.

[2] U.S. Environmental Protection Agency. Climate change indicators in the United States, Third edition. 2014. www.epa.gov/climatechange/indicators.

[3] Dechsiri C, Ghione A, Van de Wiel F, Dehling HG. 'PET Investigating of a fluidized particle: Spatial and temporal resolution and short term motion'. *Meas. Sci. Technol*.2005; (16) 851-858.

[4] Carrasco M, Ortega-Farias S. Evaluation of a model to simulate net radiation over a Vineyard cv. Cabernet Sauvignon. *Chilean journal of agricultural research*. 2008; (68):156-165.

[5] Geraldo-Ferreira A, Emilio S, Gómez-Sanchis J, Serrano-López AJ, Velázquez-Blazquez A, López-Baeza E. Modeling net radiation at surface using ''in situ'' netpyrradiometer measurements with artificial neural networks. *Expert Systems with Applications*. 2011;(38):14190–14195.

[6] Basile K, Ossénatou M, Gabin KN, Cossi NA. Dynamics and Diurnal Variations of Surface Radiation Budget over Agricultural Crops Located in Sudanian Climate. *Atmospheric and Climate Sciences.*2013;(3):121-131.

[7] Bo J, Zhang Y, Liang S, Zhang X, Xiao Z. Surface Daytime Net Radiation Estimation Using Artificial Neural Networks. *Remote Sensing*. 2014;(6):11031-11050.

[8] Mahalakshmia DV, Arati Paul DD, Ali MM, Chandra SJ, Vinay KD. Net Surface Radiation Retrieval Using Earth Observation Satellite Data and Machine Learning Algorithm. ISPRS Annals of the Photogrammetry, Remote Sensing and Spatial Information Sciences. 2014; 2(8):1-5.

[9]Santiago AV, Pereira AR, Folegatti MV, Maggiotto SR. Reference Evapotranspiration Measured with a Weighing Lysimeter and Estimated by Penman-Monteith (FAO-56) on a Monthly and Ten-Days Time Scales. *Revista Brasileira de Agrometeorologia*.2002; 10:57-66.

[10] Gavial P, Berengena J, Allen RG. Measuring versus Estimating Net Radiation and Soil Heat Flux: Impact on Penman-Monteith Reference ET Estimates in Semiarid Regions. *Agricultural Water Management.2007;(* 89): 275-286.

[11]Von Randow RCS, lvalá RCS. Estimation of Long-Wave Atmospheric Radiation over Pantanal Sul Mato Grossense during the Dry Seasons of 1999 and 2000. *Revista Brasileira de Meteorologia.2006;* 21: 398-412.

[12] Galvão JAC, Fisch G. Radiation Balance in Pasture in the Amazon. *Revista Brasileira de Agrometeorologia*.2000;(8):1-10.

[13] D'Amico G, Filippo P, Flavio P. First and second order semi-Markov chains for wind speed modeling. *Physica A.2012;* 392(5):1194-1201.

[14] Agada IO, Udochukwu BC, Sombo T. Predicting the Occurrence of Surplus and Deficit Net Radiation in Ibadan, Nigeria. *Science World Journal*.2019;14(2):1-8.

[15] Agada IO, Udochukwu BC, Utah EU. Investigating the effect of High and Low wind speed on surplus net radiation in Makurdi, Nigeria: An implication to energy imbalance. *FUDMA Journal of Sciences. 2020;* 4(1):235-245.

[16] Akinsanola AA, Ogunjobi K. Analysis of Rainfall and Temperature Variability Over Nigeria. *Global Journal of human-social science.2014;*14:65-74.

[17] Jones PD, Briffa KR. Global surface air temperature variations during the twentieth century: Part I, spatial, temporal, seasonal details. The Holocene.1992;2:165-179.

[18] Maiyza IA, Said MA, Kamel MS. Sea Surface Temperature Anomalies in the South Eastern Mediterranean Sea, *JKAU: Mar. Sci. 2001;* 21:151-159.

[19] Parker DE, Folland CK, Ward MN. Sea surface temperature anomaly pattern and prediction of seasonal rainfall in the sahelregion of Africa. In: Gregory S(ed) Recent climate change, Belhaven press, London. 1998;166-178.

[20] Varotsos CA, Efstathiou MN, Cracknell AP. On the scaling effect in global surface air temperature anomalies.*Atmos. Chem. Phy. 2013;*13: 5243–5253.

[21] John AD, William AB. Solar Engineering of Thermal Processes. Fourth Edition John Wiley &Sons,Inc. Wisconsin. 2013;138-172.

[22] Srikanthan R, McMahon TA. Stochastic generation of annual, monthly and daily climate data*: A review Hydrology and Earth System Sciences.2001;* 5(4): 653–670.

[23] Ross S. Introduction to Probability Models. Academic Press, California, 10th edition. 2010.

[24] Udom AU. Elements of Applied Mathematical Statistics. ICIDR Publishing House Akwa Ibo.2010.

[25] Echiegu EA, Ede NC, Ezenne GI. Optimization of Blaney-Morin-Nigeria (BMN) model for estimating evapotranspiration in Enugu, Nigeria *African Journal of Agricultural Research.2016;*11(20):1842-1848.

[26] Abiodun BJ, Salami AT, Tadross M. Climate Change Scenarios for Nigeria: Understanding Biophysical Impacts. Climate Systems Analysis Group, Cape Town, for Building Nigeria's Response to Climate Change (BNRCC) Project, Ibadan, Nigeria: Nigerian Environmental Study/Action Team NEST. 2011;11.

[27] Ologunorisa TE, Tersoo T. The Changing Rainfall Pattern and Its Implication for Flood Frequency in Makurdi, Northern Nigeria J. Appl. Sci. Environ. Mgt.2006;10 (3):97 – 102.

[28] Choudhary E, Vaidyanathan A. Heat stress illness hospitalizations—Environmental public health tracking program, 20 states, 2001–2010. Surveillance Summaries.2014; 63(3):1–10.

[29] Agada PO, Agada IO, Annongu WD. A Model for the Sequence of Positive and Negative Maximum Air temperature Anomaly in Port Harcourt, Nigeria Int. J. Comp. Theo.Stat. 2016;3(2):101-110.

[30] Beard CB, Eisen RJ, Barker CM, Garofalo JF, Hahn M, Hayden M, Monaghan AJ, Ogden NH, Schramm PJ. Chapter 5: Vectorborne diseases. The impacts of climate change on human health in the United States: A scientific assessment. U.S. Global Change Research Program. https://health2016.globalchange.gov. 2016.

[31] WHO, Climate Change and Human Health – Risks and Responses. Summary.2003;37.